Metabolomics Identifies Distinctive Metabolite Signatures for Measures of Glucose Homeostasis: The Insulin Resistance Atherosclerosis Family Study (IRAS-FS)

Nicholette D. Palmer,[1,2] Hayrettin Okut,[2] Fang-Chi Hsu,[3] Maggie C. Y. Ng,[1,2] Yii-Der Ida Chen,[4,5] Mark O. Goodarzi,[6] Kent D. Taylor,[4] Jill M. Norris,[7] Carlos Lorenzo,[8] Jerome I. Rotter,[4,5] Richard N. Bergman,[9] Carl D. Langefeld,[3] Lynne E. Wagenknecht,[10] and Donald W. Bowden[1,2,11]

[1]Department of Biochemistry, Wake Forest School of Medicine, Winston-Salem, North Carolina 27157; [2]Center for Genomics and Personalized Medicine Research, Wake Forest School of Medicine, Winston-Salem, North Carolina 27157; [3]Department of Biostatistical Sciences, Wake Forest School of Medicine, Winston-Salem, North Carolina 27157; [4]Institute for Translational Genomics and Population Sciences, Los Angeles Biomedical Research Institute at Harbor–University of California Los Angeles Medical Center, Torrance, California 90277; [5]Department of Pediatrics, Los Angeles Biomedical Research Institute at Harbor–University of California Los Angeles Medical Center, Torrance, California 90277; [6]Division of Endocrinology, Diabetes and Metabolism, Cedars-Sinai Medical Center, Los Angeles, California 90048; [7]Department of Epidemiology, Colorado School of Public Health, University of Colorado Denver, Aurora, Colorado 80045; [8]Department of Medicine, University of Texas Health Science Center, San Antonio, Texas 78229; [9]Department of Physiology and Biophysics, Keck School of Medicine of the University of Southern California, Los Angeles, California 90033; [10]Division of Public Health Sciences, Wake Forest School of Medicine, Winston-Salem, North Carolina 27157; and [11]Department of Internal Medicine, Wake Forest School of Medicine, Winston-Salem, North Carolina 27157

Context: Metabolomics provides a biochemical fingerprint that, when coupled with clinical phenotypes, can provide insight into physiological processes.

Objective: Survey metabolites associated with dynamic and basal measures of glucose homeostasis.

Design: Analysis of 733 plasma metabolites from the Insulin Resistance Atherosclerosis Family Study.

Setting: Community based.

Participants: One thousand one hundred eleven Mexican Americans.

Main Outcome: Dynamic measures were obtained from the frequently sampled intravenous glucose tolerance test and included insulin sensitivity and acute insulin response to glucose. Basal measures included homeostatic model assessment of insulin resistance and β-cell function.

Results: Insulin sensitivity was associated with 99 metabolites ($P < 6.82 \times 10^{-5}$) explaining 28% of the variance (R^2_{adj}) beyond 28% by body mass index. Beyond branched chain amino acids (BCAAs; $P = 1.85 \times 10^{-18}$ to 1.70×10^{-5}, $R^2_{adj} = 8.1\%$) and phospholipids ($P = 3.51 \times 10^{-17}$ to 3.00×10^{-5}, $R^2_{adj} = 14\%$), novel signatures of long-chain fatty acids (LCFAs; $P = 4.49 \times 10^{-23}$ to 4.14×10^{-7}, $R^2_{adj} = 11\%$) were observed. Conditional analysis suggested that BCAA and LCFA signatures were independent. LCFAs were not associated with homeostatic model assessment of insulin resistance

ISSN Print 0021-972X ISSN Online 1945-7197
Printed in USA

Received 5 October 2017. Accepted 7 March 2018.
First Published Online 13 March 2018

Abbreviations: AIR_g, acute insulin response to glucose; BCAA, branched-chain amino acid; BMI, body mass index; DI, disposition index; FSIGT, frequently sampled intravenous glucose tolerance test; $HOMA_B$, homeostatic model assessment of β-cell function; $HOMA_{IR}$, homeostatic model assessment of insulin resistance; IRAS-FS, Insulin Resistance Atherosclerosis Family Study; LCFA, long-chain fatty acid; PUFA, polyunsaturated fatty acid; r_S, Spearman rank-order correlation; S_G, glucose effectiveness; S_I, insulin sensitivity; T2D, type 2 diabetes.

($P > 0.024$). Acute insulin response to glucose was associated with six metabolites; glucose had the strongest association ($P = 5.68 \times 10^{-16}$). Homeostatic model assessment of β-cell function had significant signatures from the urea cycle ($P = 9.64 \times 10^{-14}$ to 7.27×10^{-6}, $R^2_{adj} = 11\%$). Novel associations of polyunsaturated fatty acids ($P = 2.58 \times 10^{-13}$ to 6.70×10^{-5}, $R^2_{adj} = 10\%$) and LCFAs ($P = 9.06 \times 10^{-15}$ to 3.93×10^{-7}, $R^2_{adj} = 10\%$) were observed with glucose effectiveness. Assessment of the hyperbolic relationship between insulin sensitivity and secretion through the disposition index revealed a distinctive signature of polyunsaturated fatty acids ($P = 1.55 \times 10^{-12}$ to 5.81×10^{-6}; $R^2_{adj} = 3.8\%$) beyond that of its component measures.

Conclusions: Metabolomics reveals distinct signatures that differentiate dynamic and basal measures of glucose homeostasis and further identifies new metabolite classes associated with dynamic measures, providing expanded insight into the metabolic basis of insulin resistance. (***J Clin Endocrinol Metab*** **103: 1877–1888, 2018)**

Type 2 diabetes (T2D) is a heterogeneous disorder characterized by hyperglycemia resulting from insulin resistance and insulin insufficiency (1). A variety of physiological measures of basal glucose homeostasis [homeostatic model assessment of insulin resistance ($HOMA_{IR}$) and homeostatic model assessment of β-cell function ($HOMA_B$)] have been widely used as clinical and epidemiological tools for estimating the degree of insulin resistance and secretory dysfunction in diverse populations (2, 3). However, dynamic measures of glucose homeostasis obtained from euglycemic–hyperinsulinemic and hyperglycemic clamps (4) are considered the "gold standard" for assessment of insulin resistance and β-cell dysfunction. These measures are highly correlated with results obtained from the frequently sampled intravenous glucose tolerance test [FSIGT; insulin sensitivity index (S_I) and acute insulin response to glucose (AIR_g)] across a range of glucose tolerance states (5–8). These dynamic measures could be considered physiologically more proximal to pathogenic components of T2D and provide insight into the discrete mechanisms of action (9).

High-throughput assessment of small-molecule intermediates in biological systems, termed metabolomics, provides a valuable tool for understanding biochemical pathways and disease mechanisms (10). Early studies in this field have frequently targeted specific metabolite classes, for example, amino acids, acylcarnitines, and organic acids. When applied to T2D, targeted metabolomic studies have revealed a characteristic metabolomic signature of amino acids, especially increased branch-chain amino acids (BCAAs), being associated with insulin resistance and overt disease. Thus, increased levels of leucine, isoleucine, valine, phenylalanine, and tyrosine were associated with up to a fivefold risk for future T2D (11–13). As technology has evolved, broad-spectrum evaluation of metabolomic features has become increasingly feasible. Metabolomic studies of the overt phenotype of T2D have reported alterations in amino acid, lipid, and sugar metabolites associated with disease (11, 14). However, large-scale metabolomic studies of alterations preceding overt disease, simultaneously assessing both dynamic and basal measures of glucose homeostasis, have not been undertaken.

The goal of this study was to provide a comprehensive survey of the metabolomic signatures of dynamic measures of glucose homeostasis using metabolomic profiling (n = 733 metabolites) in Mexican American participants from the Insulin Resistance Atherosclerosis Family Study (IRAS-FS). These results were then contrasted with findings from basal indices of glucose homeostasis in the same study population. These results reveal distinctive metabolic patterns associated with different measures of glucose homeostasis.

Materials and Methods

Study population

The IRAS-FS was designed to investigate the genetic and environmental basis of glucose homeostasis and visceral adiposity. Study design, recruitment, and phenotyping have been previously described (15). Specific to this report, Mexican American families were recruited from clinical centers in San Antonio, TX and San Luis Valley, CO. The study protocol was approved by the Institutional Review Board of each participating clinical and analysis site and all participants provided their written informed consent.

Phenotyping

A clinical examination was performed for nondiabetic participants that included an interview, an FSIGT, anthropometric measurements, and blood collection. Dynamic measures of glucose homeostasis included those from the FSIGT using the reduced sampling protocol (16–18) calculated by mathematical modeling methods (MINMOD) (9), including the S_I index and glucose effectiveness (S_G). Additionally, AIR_g was calculated as the increase in insulin concentrations at 2 to 8 minutes above the basal (fasting) insulin level after a bolus glucose injection at 0 to 1 minute. Disposition index (DI) was calculated as the product of $S_I \times AIR_g$. $HOMA_{IR}$ and $HOMA_B$ were modeled from fasting glucose and insulin measures using the updated HOMA model (19).

Metabolite profiling of fasting plasma samples stored at −80°C since baseline collection from 1999 to 2002 was performed. Detection and quantification of 1274 metabolites was completed by Metabolon (Durham, North Carolina) using untargeted liquid chromatography–mass spectrometry (DiscoveryHD4 panel). This panel identifies and provides relative quantitation for known chemical compounds (n = 733) among amino acid, carbohydrate, energy, lipid, nucleotide, and peptide superpathways, which were the focus of this report. Prior to receipt, data were block corrected for run day, normalized by batch, and missing data by metabolite was imputed to the minimum. Subsequently, sample-level analysis revealed an excess of metabolite outliers (±4 standard deviations) for a single sample (n = 134 outliers), which was removed from analysis. Individual metabolite values were winsorized at 1% and 99% to reduce the effect of outliers. Correlation structure among metabolites was examined using a Spearman rank-order correlation (r_S).

Statistical analysis

Variance component models as implemented in SOLAR (20) were used to test for association between metabolites and glucose homeostasis phenotypes accounting for the familial relationships using a random effect model. All models were adjusted for age, sex, body mass index (BMI), and recruitment center. For glucose homeostasis traits, winsorization and/or transformation was applied to best approximate the distributional assumptions of conditional normality and homogeneity of the variance. Transformations included natural logarithm of the trait plus a constant (S_I), square root (AIR_g and DI), and natural logarithm ($HOMA_{IR}$, $HOMA_B$, and fasting insulin). S_G and fasting glucose were not transformed. Tests of association between individual metabolites (predictor) and glucose homeostasis phenotypes (outcome) were computed using the Wald test. A conservative Bonferroni correction was used to account for multiple testing with 733 metabolites, that is, 6.82×10^{-5} (0.05/733). To test for independent associations, conditional models with inclusion of metabolites as covariates were evaluated. A random effects model as computed in SOLAR was used to estimate the proportion of variance (R^2) explained by metabolites within a given subpathway after removing the effect of covariates. Correction of this value for the total number of samples and metabolites in a subpathway was also performed (R^2_{adj}).

To evaluate the cumulative effect of associated metabolites on a given phenotype, the random effects model was used as implemented in SOLAR. R^2 was estimated in a model including the minimum number of covariates, that is, age, sex, and recruitment center. Subsequently, models were constructed inclusive of BMI with and without all individually associated metabolites.

Results

This study sample comprised data from up to 1111 Mexican Americans from the IRAS-FS cohort (Table 1). Sample sizes were nominally different between dynamic (n = 922) and basal (n = 940) measures owing to the ease of sample collection for the latter. On average, study subjects were overweight (BMI = 28.9 kg/m^2) and most participants were female. Participants had a mean S_I of $2.16 \pm 1.85 \times 10^{-4}$ min/μU/mL, mean AIR_g of 777 ± 665 μU/mL/min, and a resulting mean DI of 1339 ± 1227. Fasting glucose levels (93.2 ± 9.4 mg/dL) were consistent with a nondiabetic population. Basal estimates of insulin resistance from $HOMA_{IR}$ were 1.66 ± 1.03 and estimates of β-cell function from $HOMA_B$ were 121.2 ± 46.9. The heritability estimates and genetic and environmental correlations for these phenotypes have been published previously (21).

Table 1. Clinical Characteristics of the IRAS-FS Cohort

	Values
Demographics	
Sample size	1111
Age, y	42.3 ± 13.9
Women, %	59.0
BMI, kg/m^2	28.9 ± 6.2
Dynamic measures	
S_I, x 10^{-4} min/μU/mL	2.16 ± 1.85
S_G, per min	0.021 ± 0.009
AIR_g, μU/mL/min	777 ± 665
DI	1339 ± 1227
Basal measures	
Fasting glucose, mg/dL	93.2 ± 9.4
Fasting insulin, mL/U/L	14.8 ± 10.6
$HOMA_{IR}$	1.66 ± 1.03
$HOMA_B$	121.2 ± 46.9

Values are expressed as the mean and standard deviation unless otherwise indicated.

Association analysis of dynamic and basal measures of S_I revealed some common features but also distinct differences in metabolite profiles. Analysis of S_I (dynamic measure) and $HOMA_{IR}$ (basal measure) revealed significant association with 152 metabolites, approximately half of which were unique to each phenotype (Fig. 1). Consistent with previous reports, both dynamic and basal measures were associated with leucine, isoleucine, and valine metabolism, metabolites involved in BCAA metabolism (Fig. 2; Table 2). Taken together, significant BCAA metabolites explained 8.1% to 10% of the variance and were inversely associated with S_I. The strongest association was detected at 3-methyl-2-oxovalerate for S_I ($\beta = -0.55$, $P = 1.85 \times 10^{-18}$; Supplemental Table 2A) and $HOMA_{IR}$ ($\beta = 0.54$, $P = 1.57 \times 10^{-14}$; Supplemental Table 2B). The most strongly associated metabolite signature with S_I was long-chain fatty acid (LCFA) metabolism (Fig. 2A; Table 2), which was also inversely associated with S_I. Specifically, the most significant metabolites were stearate ($\beta = -0.70$, $P = 4.49 \times 10^{-23}$), margarate ($\beta = -0.36$, $P = 1.72 \times 10^{-17}$), and palmitate ($\beta = -0.44$, $P = 4.42 \times 10^{-15}$), metabolites that were highly correlated with one another ($r_S > 0.79$, Supplemental Table 1). Analysis conditioned on the most

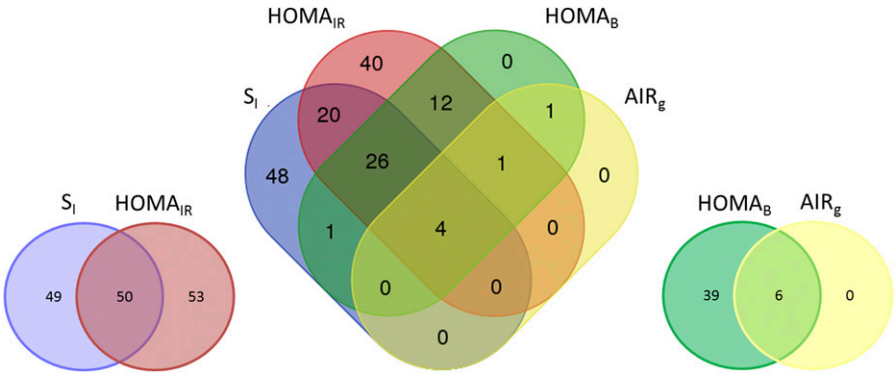

Figure 1. Overlap of significant metabolites between dynamic and basal measures of glucose homeostasis.

significant BCAA metabolite (3-methyl-2-oxovalerate) that captured the effect of additional BCAA metabolites ($r_S > 0.56$) did not significantly impact the observed LCFA associations with S_I ($P = 4.18 \times 10^{-19}$ to 2.00×10^{-7}; Supplemental Table 4), suggesting that the BCAA and LCFA associations were independent. Comparatively, association with HOMA$_{IR}$ was much less pronounced ($P > 0.069$) and the only LCFA metabolite significantly associated with HOMA$_{IR}$ was myristoleate ($\beta = -0.15$, $P = 3.22 \times 10^{-7}$), which was not associated with S_I ($\beta = -0.04$, $P = 0.13$) (Supplemental Fig. 1; Supplemental Table 2). Results for fasting insulin were largely similar to HOMA$_{IR}$ and are presented in Supplemental Table 3G.

Examination of dynamic and basal measures of insulin secretion also revealed differences in metabolite profiles for AIR$_g$ and HOMA$_B$ (Fig. 1). Examination of AIR$_g$, a dynamic measure of insulin secretion, revealed significant association with only 6 metabolites compared with 45 metabolites significantly associated with HOMA$_B$ (Fig. 2B). By far, the most prominent was association of AIR$_g$ with glucose ($\beta = -26.57$, $P = 5.68 \times 10^{-16}$, $R^2_{adj} = 4.0\%$; Supplemental Table 3C). Noticeably less striking for HOMA$_B$ was association with glucose ($\beta = -0.42$, $P = 5.40 \times 10^{-5}$; Supplemental Fig. 1; Supplemental Table 2D). Among HOMA$_B$-associated pathways, γ-glutamyl amino acid ($P = 1.88 \times 10^{-9}$ to 5.10×10^{-5}, $R^2_{adj} = 13\%$) and urea cycle ($P = 9.64 \times 10^{-14}$ to 7.27×10^{-6}, $R^2_{adj} = 11\%$) metabolism individually explained the largest proportion of variance (Table 2). Results for fasting glucose were largely similar to HOMA$_B$ (Supplemental Table 3H).

Analysis of data derived from the FSIGT facilitates capture of the ability of glucose to enhance its own disposal, termed glucose effectiveness (S_G). Metabolomic analysis of S_G (Fig. 2C; Supplemental Table 3E) identified significant association with 47 metabolites. Consistent with this measurement, S_G was not significantly associated with glucose ($\beta = -0.0096$, $P = 3.42 \times 10^{-4}$). The most prominent pathways were identified within lipid metabolism and included polyunsaturated fatty acid [(PUFA) $P = 2.58 \times 10^{-13}$ to 6.70×10^{-5}, $R^2_{adj} = 10\%$] and LCFA ($P = 9.06 \times 10^{-15}$ to 3.93×10^{-7}, $R^2_{adj} = 9.8\%$) metabolism. Beyond S_G, the FSIGT analysis also captures the interrelationship of S_I and secretion through the DI, which captures the compensatory response of β-cells to insulin resistance to maintain glucose homeostasis. Perhaps surprising, given that DI is the product of S_I and AIR$_g$, distinct metabolites appear to be more strongly associated with this composite phenotype; that is, 18 of 56 significant metabolites were unique to DI (Fig. 2D; Supplemental Fig. 1; Supplemental Table 3F). In addition to BCAA ($P = 6.99 \times 10^{-13}$ to 6.10×10^{-5}, $R^2_{adj} = 5.6\%$) and LCFA ($P = 6.23 \times 10^{-14}$ to 3.63×10^{-6}, $R^2_{adj} = 3.9\%$) metabolism, there was a strong association with PUFA metabolism ($P = 1.55 \times 10^{-12}$ to 5.81×10^{-6}, $R^2_{adj} = 3.8\%$), which was more modestly associated with S_I ($P = 2.36 \times 10^{-10}$ to 3.30×10^{-5}) and absent from association with AIR$_g$ ($P > 4.73 \times 10^{-3}$). Among the 56 DI-associated metabolites were glycolysis, gluconeogenesis, and pyruvate metabolism ($P = 1.94 \times 10^{-21}$ to 2.00×10^{-5}, $R^2_{adj} = 8.3\%$), inclusive of glucose ($\beta = -45.18$, $P = 1.90 \times 10^{-21}$).

Although fasting measures of insulin and glucose are used to calculate basal measures of insulin resistance (HOMA$_{IR}$) and secretion (HOMA$_B$), association analysis of metabolites with fasting insulin and fasting glucose were also examined. Fasting insulin was significantly associated with 79 metabolites (Supplemental Table 3G). Overrepresented pathways included BCAA ($P = 7.67 \times 10^{-12}$ to 4.10×10^{-5}, $R^2_{adj} = 11\%$), plasmalogen ($P = 1.67 \times 10^{-16}$ to 3.90×10^{-5}, $R^2_{adj} = 11\%$), and glycolysis, gluconeogenesis, and pyruvate ($P = 6.30 \times 10^{-12}$ to 1.74×10^{-7}, $R^2_{adj} = 13\%$) metabolism. Fasting glucose was significantly associated with 26 metabolites (Supplemental Table 3H). Not surprisingly, it was significantly associated with glycolysis, gluconeogenesis, and pyruvate metabolism ($P = 3.88 \times 10^{-91}$ to 1.90×10^{-5}, $R^2_{adj} = 39\%$).

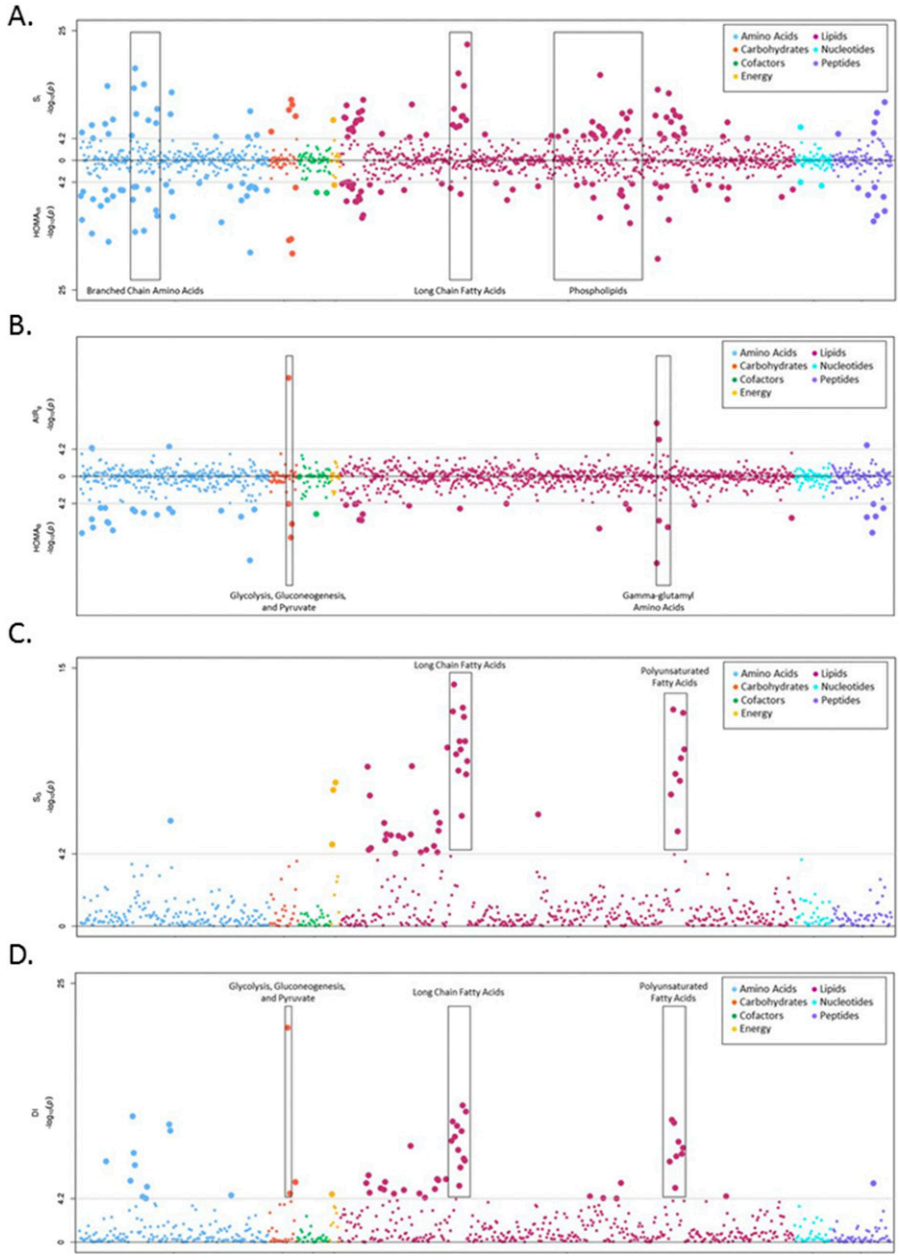

Figure 2. (A) Opposed plot of metabolite associations with S_I and $HOMA_{IR}$. Log-transformed *P* values are shown for association with S_I (top) and $HOMA_{IR}$ (bottom). Metabolites are plotted by superpathway: amino acids (blue), carbohydrates (orange), cofactors and vitamins (green), energy (yellow), lipids (pink), nucleotides (turquoise), and peptides (purple). The gray lines correspond to statistical significance ($P < 6.82 \times 10^{-5}$, corrected for 733 metabolites) in each direction. (B) Opposed plot of metabolite associations with AIR_g and $HOMA_B$. Log-transformed *P* values are shown for association with AIR_g (top) and $HOMA_B$ (bottom). Metabolites are plotted by superpathway: amino acids (blue), carbohydrates (orange), cofactors and vitamins (green), energy (yellow), lipids (pink), nucleotides (turquoise), and peptides (purple). The gray lines correspond to statistical significance ($P < 6.82 \times 10^{-5}$, corrected for 733 metabolites) in each direction. (C) Manhattan plot of metabolite associations with S_G. Log-transformed *P* values are shown for association with S_G. Metabolites are plotted by superpathway: amino acids (blue), carbohydrates (orange), cofactors and vitamins (green), energy (yellow), lipids (pink), nucleotides (turquoise), and peptides (purple). The gray lines correspond to statistical significance ($P < 6.82 \times 10^{-5}$, corrected for 733 metabolites). (D) Manhattan plot of metabolite associations with DI. Log-transformed *P* values are shown for association with DI. Metabolites are plotted by superpathway: amino acids (blue), carbohydrates (orange), cofactors and vitamins (green), energy (yellow), lipids (pink), nucleotides (turquoise), and peptides (purple). The gray lines correspond to statistical significance ($P < 6.82 \times 10^{-5}$, corrected for 733 metabolites).

To examine the cumulative impact of all significantly associated metabolites with the phenotypes of interest, the proportion of variance explained was calculated with and without the inclusion of BMI or individually associated metabolites (Table 3). Across the eight dynamic and basal glucose homeostasis phenotypes examined, essential covariates, that is, age, sex, and recruitment center, explained a limited proportion of the variance ($R^2_{adj} < 12\%$). These estimates were further increased with the inclusion of BMI ($R^2_{adj} < 35\%$). However, the

Table 2. Significant Associations ($R^2_{adj} > 0.10$) Among Metabolites With Measures of Insulin Resistance (S_I and $HOMA_{IR}$) and Insulin Secretion (AIR_g and $HOMA_B$)

Superpathway	Subpathway	n[a]	n[b]	Metabolites[c]	*P* Value Range	R^2_{adj}[d]
S_I (n_{max} = 922)						
Lipid	LCFA	10	14	Stearate (18:0), margarate (17:0), palmitate (16:0), 10-nonadecenoate (19:1n9), oleate/vaccenate (18:1), nonadecanoate (19:0), pentadecanoate (15:0), 10-heptadecenoate (17:1n7), myristate (14:0), eicosenoate (20:1)	4.49×10^{-23} to 4.14×10^{-7}	0.11
Lipid	Phospholipid metabolism	18	82	1-Palmitoyl-2-linoleoyl-GPI (16:0/18:2), 1-stearoyl-2-oleoyl-GPE (18:0/18:1), 1-stearoyl-2-docosahexaenoyl-GPE (18:0/22:6)[e], 1-stearoyl-2-linoleoyl-GPE (18:0/18:2)[e], 1-palmitoyl-2-arachidonoyl-GPI (16:0/20:4)[e], 1-palmitoyl-2-linoleoyl-GPE (16:0/18:2), 1-palmitoyl-2-oleoyl-GPE (16:0/18:1), 1-stearoyl-2-linoleoyl-GPI (18:0/18:2), **1-linoleoyl-2-docosapentaenyol-GPC (18:2/22:5n3)[e]**, 1-stearoyl-2-dihomo-linolenoyl-GPC (18:0/20:3n3 or 6)[e], 1-palmitoyl-2-palmitoleoyl-GPE (16:0/16:1)[e], 1-palmitoyl-2-arachidonoyl-GPE (16:0/20:4)[e], 1-stearoyl-2-arachidonoyl-GPE (18:0/20:4), 1-palmitoyl-2-dihomo-linolenoyl-GPC (16:0/20:3n3 or 6)[e], 1-palmitoyl-2-palmitoleoyl-GPC (16:0/16:1)[e], **1-oleoyl-2-docosapentaenoyl-GPC (18:1/22:5n3)[e]**, **1,2-dilinoleoyl-GPC (18:2/18:2)**, 1-stearoyl-2-adrenoyl-GPC (18:0/22:4)[e]	3.51×10^{-17} to 3.00×10^{-5}	0.14
Peptide	γ-Glutamyl amino acid	4	16	γ-glutamylvaline, γ-glutamylisoleucine[e], **γ-glutamylglycine**, **γ-glutamylglutamine**	6.03×10^{-12} to 5.69×10^{-6}	0.10
$HOMA_{IR}$ (n_{max} = 940)						
Amino acid	Alanine and aspartate metabolism	3	6	Asparagine, **alanine**, **aspartate**	3.29×10^{-12} to 9.16×10^{-7}	0.11
Amino acid	Glycine, Serine and Threonine Metabolism	4	9	*N*-acetylglycine, serine, glycine, betaine	2.00×10^{-16} to 1.95×10^{-6}	0.11
Amino acid	Leucine, isoleucine and valine metabolism	7	24	**Isoleucine, 3-methyl-2-oxovalerate, valine, 3-hydroxyisobutyrate, e-methyl-2-oxobutyrate, leucine, 4-methyl-2-oxopentanoate**	1.57×10^{-14} to 8.32×10^{-6}	0.10
Amino acid	Urea cycle; arginine and proline metabolism	5	18	**2-Oxoarginine, proline, arininate**, dimethylarginine, citrulline	1.68×10^{-18} to 1.00×10^{-5}	0.13
Carbohydrate	Glycolysis, gluconeogenesis, and pyruvate metabolism	3	7	**Pyruvate, glucose, lactate**	1.06×10^{-18} to 6.54×10^{-16}	0.11
Lipid	Phospholipid metabolism	11	82	**1-Stearoyl-2-oleoyl-GPE (18:0/18:1), 1-palmitoyl-2-linoleoyl-GPI (16:0/18:2), 1-stearoyl-2-linoleoyl-GPE (18:0/18:2)[e], 1-stearoyl-2-docosahexaenoyl-GPE (18:0/22:6)[e], 1-palmitoyl-2-dihomo-linolenoyl-GPC (16:0/20:3n3 or 6)[e], 1-stearoyl-2-dihomo-linolenoyl-GPC (18:0/20:3n3 or 6)[e],** choline, **1-myristoyl-2-palmitoyl-GPC (14:0/16:0),** arachidonoylcholine, 1-oleoyl-2-docosapentaenoyl-GPC (18:1/22:5n3)[e], **1-palmitoyl-2-arachidonoyl-GPI (16:0/20:4)[e], 1-palmitoyl-2-arachidonoyl-GPI (16:0/20:4)[e]**	6.35×10^{-12} to 5.50×10^{-5}	0.11

(*Continued*)

Table 2. Continued

Superpathway	Subpathway	n[a]	n[b]	Metabolites[c]	*P* Value Range	R^2_{adj}[d]
Peptide	γ-Glutamyl amino acid	7	16	γ-Glutamylglutamine, **γ-glutamylisoleucine[e]**, **γ-glutamylvaline**, **γ-glutamyltyrosine**, γ-glutamyl-2-aminobutyrate, γ-glutamylglycine, **γ-glutamylglutamate**	1.74×10^{-12} to 6.80×10^{-5}	0.16
$HOMA_B$ (n_{max} = 940)						
Amino acid	Urea cycle; arginine and proline metabolism	2	18	**2-Oxoarginine**, citrulline	9.64×10^{-14} to 7.27×10^{-6}	0.11
Peptide	γ-Glutamyl amino acid	5	16	γ-Glutamylglutamine, γ-glutamyl-2-aminobutyrate, **γ-glutamylisoleucine**, **γ-glutamylvaline**, **γ-glutamylglycine**	1.88×10^{-9} to 5.10×10^{-5}	0.13

[a]Number of significant metabolites ($P < 6.82 \times 10^{-5}$).

[b]Total number of metabolites in the specified subpathway.

[c]Metabolites in bold had a positive β value (direction of effect).

[d]Proportion of variance explained after adjusting for the number of associated metabolites in each subpathway.

[e]Named compounds identified from mass and fragmentation analysis but yet to be confirmed with standards.

proportion of variance explained by significantly associated metabolites consistently exceeded that of BMI when included in the models. For example, 6.4% of the variance in S_I was explained in a model including age, sex, and recruitment center. This estimate increased to 35% and 63% with the inclusion of BMI and BMI with significant metabolites (n = 99), respectively. Similar estimates were observed for $HOMA_{IR}$. For insulin secretion, 7.3% of the variance in AIR_g was explained in a model including age, sex, and recruitment center. This estimate increased to 11% and 21% with the inclusion of BMI and BMI with significant metabolites (n = 6), respectively. A larger proportion of the variance was explained for $HOMA_{IR}$, with BMI explaining 19% and BMI with significant metabolites (n = 45) explaining 45%.

Discussion

Using metabolomics, we have performed a survey of the signatures of dynamic and basal measures of glucose homeostasis. Qualitatively there were many more metabolites associated with S_I suggesting metabolic complexity of this measure when compared with insulin secretion (Fig. 1). Assessment of insulin response revealed similar numbers of metabolites significantly associated with S_I and $HOMA_{IR}$, although overlapping metabolites were more significantly associated with S_I. These observations suggest a complex physiology where the findings from basal and dynamic measures of glucose homeostasis share commonality but where a more comprehensive phenotypic assessment, beyond basal measures routinely assessed in large epidemiologic studies, may provide more insight into the contributing pathways. When placed in the context of genetic studies, these observations suggest a complex physiology may underlie the dearth of genetic associations for insulin resistance.

A closer examination of the metabolites associated with S_I revealed signatures of branched-chain amino acid (BCAA; R^2_{adj} = 8.1% to 10%) and phospholipid (R^2_{adj} = 11% to 14%) metabolism. The signature of dysregulated BCAA metabolism is a well-documented finding from targeted metabolomics studies in the setting of insulin resistance (13) and T2D where elevated levels predict disease development (11). The findings in the present study point to the intermediate metabolites in BCAA catabolism generated after the rate-limiting step catalyzed by branched-chain aminotransferase, that is, 3-methyl-2-oxovalerate from isoleucine, 3-methyl-2-oxobutyrate from valine, and 4-methyl-2-oxopentanoate from leucine. Consistent with our findings, 3-methyl-2-oxovalerate has been implicated as a predictive biomarker for insulin resistance as assessed via the hyperinsulinemic–euglycemic clamp (22). Beyond metabolites associated with overt disease, mannose (23) and α-hydroxybutyrate (22) have been identified as early biomarkers of insulin resistance. In the IRAS-FS, mannose was not associated with dynamic (S_I; $\beta = -0.10$, $P = 0.089$) or basal ($HOMA_{IR}$; $\beta = 0.14$, $P = 0.032$) measures of insulin response. In contrast, α-hydroxybutyrate was significantly associated with S_I ($\beta = -0.21$, $P = 1.27 \times 10^{-9}$) but not $HOMA_{IR}$ ($\beta = 0.05$, $P = 0.21$).

Novel to this study is the strong association of LCFAs with S_I in this nondiabetic cohort. In comparison with BCAAs, LCFAs were individually more strongly associated and cumulatively accounted for a greater proportion

Table 3. Proportion of Variance (R^2_{adj}) Explained by Demographics and/or Metabolites for Measures of Glucose Homeostasis

	R^2_{adj}
S_I (n = 922)	
Age, sex, center	0.064
Age, sex, center, BMI	0.35
Age, sex, center, BMI, metabolites (n = 99, $P < 6.82 \times 10^{-5}$)	0.63
$HOMA_{IR}$ (n = 940)	
Age, sex, center	0.0064
Age, sex, center, BMI	0.29
Age, sex, center, BMI, metabolites (n = 103, $P < 6.82 \times 10^{-5}$)	0.63
AIR_g (n = 922)	
Age, sex, center	0.073
Age, sex, center, BMI	0.11
Age, sex, center, BMI, metabolites (n = 6, $P < 6.82 \times 10^{-5}$)	0.21
$HOMA_B$ (n = 940)	
Age, sex, center	0.024
Age, sex, center, BMI	0.19
Age, sex, center, BMI, metabolites (n = 45, $P < 6.82 \times 10^{-5}$)	0.45
S_G (n = 922)	
Age, sex, center	0.047
Age, sex, center, BMI	0.14
Age, sex, center, BMI, metabolites (n = 47, $P < 6.82 \times 10^{-5}$)	0.27
DI (n = 922)	
Age, sex, center	0.12
Age, sex, center, BMI	0.21
Age, sex, center, BMI, metabolites (n = 56, $P < 6.82 \times 10^{-5}$)	0.36
Fasting insulin (n = 979)	
Age, sex, center	0.0033
Age, sex, center, BMI	0.23
Age, sex, center, BMI, metabolites (n = 79, $P < 6.82 \times 10^{-5}$)	0.56
Fasting glucose (n = 981)	
Age, sex, center	0.12
Age, sex, center, BMI	0.22
Age, sex, center, BMI, metabolites (n = 26, $P < 6.82 \times 10^{-5}$)	0.64

of variance. Additionally, analysis conditioned on association with BCAAs did not significantly impact the associations observed with LCFAs. Patients with T2D often present with dyslipidemia and LCFAs are reported to be elevated in the setting of impaired glucose tolerance (22, 24–26). In this study, S_I was inversely correlated among all LCFAs assessed (n = 14) with the most significant saturated fatty acids including stearate ($\beta = -0.70$, $P = 4.49 \times 10^{-23}$), margarate ($\beta = -0.36$, $P = 1.72 \times 10^{-17}$), and palmitate ($\beta = -0.44$, $P = 4.42 \times 10^{-15}$). Because S_I is a measure of peripheral insulin resistance, these associations could reflect metabolic inflexibility, that is, lipid oxidation that is not proportional to lipid availability, which can result in accumulation of lipid in peripheral tissues, leading to insulin resistance (27). In this nondiabetic cohort, increased levels of LCFAs present in individuals with lower S_I values do not appear to contribute to lipotoxicity in the β-cells, as LCFAs were not associated with measures of insulin secretion as is seen in the setting of T2D (28). Notably, LCFAs associated with S_I were not significantly associated with the basal measure of insulin resistance, $HOMA_{IR}$. This observation suggests that basal measures of insulin resistance that are used broadly in the literature owing to their ease of assessment may not fully capture the physiological pathways involved in disease risk; that is, $HOMA_{IR}$ is a measure of hepatic insulin resistance as compared with S_I, which measures peripheral S_I (29).

In comparison with S_I, there were fewer metabolites associated with insulin secretion. $HOMA_B$, the basal measure of insulin secretion, was significantly associated with 45 metabolites. Overrepresented pathways included γ-glutamyl amino acid and urea cycle metabolism. γ-Glutamyl amino acids have previously been thought to impact insulin resistance as a product of glutathione degradation (30). However, in this study we observe an association with insulin secretion with five significant and nominally correlated (r_S = 0.24 to 0.79) metabolites (γ-glutamylglutamine, γ-glutamyl-2-aminobutyrate, γ-glutamylisoleucine, γ-glutamylvaline, γ-glutamylglucine). Similarly, two uncorrelated metabolites (r_S = 0.09) in the urea cycle were associated with $HOMA_B$. The most significant metabolite, 2-oxoargnine ($\beta = 0.13$, $P = 9.64 \times 10^{-14}$), was positively associated with $HOMA_B$ whereas citrulline ($\beta = -0.32$, $P = 7.27 \times 10^{-6}$) was inversely associated. Whereas arginine has been shown to promote insulin secretion (31), the conversion of arginine to citrulline produces nitric oxide, which negatively impacts insulin secretion (32). Also, although currently there are no detailed studies of arginine metabolism in the β-cell, the observation that 2-oxoargnine was positively associated with insulin secretion could be mechanistically related to the results with citrulline whereby the conversion of arginine to 2-oxoargnine diverts from a nitric oxide–producing pathway. Among additional urea cycle metabolites examined (n = 18), levels of asymmetric dimethylarginine are reported to be elevated in T2D (33) with its underlying contribution through insulin resistance (34). In this study, we report an inverse association with $HOMA_B$ in which elevated levels of dimethylarginine were associated with decreased β-cell function ($\beta = -0.32$, $P = 1.37 \times 10^{-4}$). Parenthetically, this metabolite was also associated with $HOMA_{IR}$ ($\beta = -0.56$, $P > 3.17 \times 10^{-6}$), although the inverse relationship would suggest that metabolite levels were decreased in the presence of insulin resistance; however, in the present study we could not differentiate between symmetric and asymmetric dimethylarginine.

The metabolomic complexity of measures of insulin resistance compared with measures of insulin secretion may be reflected in genetic analyses performed to date in

which loci associated with the β-cell greatly outnumber variants associated with S_I (35). The underlying metabolic complexity of S_I suggests challenges to finding genetic loci through simply searching for association with T2D. Genetic analysis of the metabolite subgroups (*e.g.*, BCAA, LCFA) may be fruitful in the future.

Novel to this study and reflective of the clinical assessment of glucose metabolism is capturing the ability of glucose to enhance its own disposal, that is, S_G. Studies have suggested that S_G is an important determinant of T2D onset owing to the increased dependence on glucose-mediated glucose disposal when there is dysregulation of S_I and secretion (36). Metabolite signatures associated with S_G included PUFA and LCFA metabolism, signatures initially observed with S_I. Among PUFA metabolites, the strongest associations included signals for linoleate ($\beta = -0.0068$, $P = 4.04 \times 10^{-13}$) and linolenate ($\beta = -0.0044$, $P = 5.31 \times 10^{-11}$), which are two essential fatty acids. Importantly, although these signals were inversely associated with S_G, note that PUFA metabolites farther down the pathway, for example, arachidonic acid and docosapentaenoate that contribute to proinflammatory phenotypes and eicosapentaenoate and docosahexaenoate that contribute to anti-inflammatory phenotypes, were not significantly associated. The potential for diversion of products of linoleate and linolenate metabolism can be seen through the significant association of docosatrienoate (22:3n6) ($\beta = -0.00080$, $P = 1.75 \times 10^{-10}$), docosadienoate ($\beta = -0.0049$, $P = 1.42 \times 10^{-9}$), and docosatrienoate (22:3n3) ($\beta = -0.0021$, $P = 3.62 \times 10^{-9}$). Docosatrienoates (22:3n3 and 22:3n6) are rare PUFAs resulting from the production of pinolenic acid, which has been shown to increase glucagon-like peptide-1 and suppress appetite (37). Although pinolenic acid was directly assessed herein, the association of metabolites downstream could suggest a mechanism of action; for example, low levels of downstream metabolites suggest utilization of pinolenic acid, resulting in improvements in glucose homeostasis. It is also worth noting that docosadienoate has been shown to suppress ghrelin secretion, a gastric peptide hormone controlling appetite and energy homeostasis (38). Therefore, increased levels of docosadienoate, associated with decreased S_G, would suppress ghrelin secretion and promote appetite. It is possible that reliance on the pathways captured by S_G are somewhat reduced in this nondiabetic cohort; that is, glucose tolerance is a function of insulin secretion, insulin action, and S_G and is maintained in normoglycemic individuals through a compensatory increase in insulin secretion. Therefore, the variability of S_G among participants was quite small ($S_G = 0.021 \pm 0.009$), reducing the power to detect effects for this trait.

In addition to S_G, the FSIGT provides an ability to examine the hyperbolic relationship that exists between S_I and AIR_g in the form of DI. Generally considered a β-cell parameter, DI represents the ability of β-cells to compensate for insulin resistance. Consistent with component phenotypes, attenuated association with BCAA and LCFA metabolism was observed likely owing to a lack of association with AIR_g. Among more significantly associated metabolites were those capturing PUFA metabolism that were modestly less significant and far less prominent with S_I. All PUFAs were negatively correlated with DI and represented both omega-3 and omega-6 fatty acids, including three essential fatty acids (α-linolenate, $\beta = -7.38$, $P = 7.87 \times 10^{-10}$; linoleate, $\beta = -10.04$, $P = 3.02 \times 10^{-9}$; and docosahexaenoate, $\beta = -5.18$, $P = 5.81 \times 10^{-6}$). From the literature, dietary omega-3 fatty acids are thought to be anti-inflammatory, although the contribution to diabetes remains unclear (39). For omega-6 fatty acids, the contribution to overt T2D remains contentious. In a recent report, higher proportions of linoleic acid, but not arachidonic acid, were associated with a lower risk of developing T2D (40). Although these results may seem inconsistent with the results reported in the present study, this publication examined these biomarkers as a percentage of total fatty acids. Moreover, the current observations are from a normoglycemic cohort where, compensatory with increasing insulin resistance, insulin secretion increases prior to development of overt disease (41). It is also noteworthy that docosadienoate (22:2n6) was inversely associated with DI and represents a shunting from the omega-6 pathway.

It is striking that metabolites contribute a large proportion of variance for multiple traits, especially S_I. Furthermore, it is notable that BMI, often referred to as the driver of insulin resistance, explains a more nominal proportion of the variance for S_I (Table 3), consistent with our prior research in the IRAS-FS. We observed that among glucose homeostasis measures, a model inclusive of demographic characteristics (age, sex, recruitment center), BMI, and significant metabolites, on average, explained twice the proportion of variance as did a model including demographic characteristics and BMI alone; taken together, these accounted for 63% of the variance in S_I. When considered in the context of dynamic measures, these results suggest that metabolomic biomarkers have the potential to be surrogates, that is, they can be used to impute measures from expensive and difficult-to-obtain phenotypes in large epidemiological cohorts. This would benefit both epidemiological and genetic mapping studies. Future clinical models may benefit from the assessment of metabolites to improve risk prediction.

Whereas the current study recapitulates previously observed signatures associated with insulin resistance and

T2D, it has also identified novel metabolites for glucose homeostasis. However, it is not without its limitations. The primary limitation of most studies is the ability to detect and replicate an effect, that is, power. In the present study using a stringent Bonferroni correction, there was >80% power to detect contributions of 2.6% to 2.9% of the variance for the phenotypes examined using univariate models. Moreover, based on the ethnicity of the participants, their family structure, and the sophistication of metabolic phenotyping, replication of these findings in a comparable sample is currently not possible. The dataset investigated in the present study was untargeted acquisition of data. This approach, which relies on liquid chromatography–mass spectrometry, could be complemented by other mass spectrometry approaches (*e.g.*, gas chromatography–mass spectrometry, and extended across other platforms (*e.g.*, nuclear magnetic resonance spectroscopy). Phenotypically, the present research examined the association of metabolites with both dynamic and basal cross-sectional measures of glucose homeostasis. Notably, there are additional dynamic measures of glucose homeostasis that could provide further insight such as the oral glucose tolerance test, which could provide insight into gut hormone signaling, for example, incretin pathways. Additionally, the cross-sectional measurement of both metabolites and measures of glucose homeostasis precludes direct insight into a causal or consequential relationship between these variables, although the results are hypothesis generating for future studies.

In summary, metabolomic analysis reveals distinct signatures that differentiate dynamic and basal measures of glucose homeostasis, providing unique insight into the pathophysiology of metabolic disease. Significant observations appeared to be more prominent among measures of insulin resistance, implicating BCAA, phospholipid, and LCFA metabolism. In contrast, signatures of insulin secretion were fewer in number but highlighted a contribution from the urea cycle in basal measures. Capturing the hyperbolic relationship between insulin resistance and secretion, DI was associated with novel signatures from PUFA metabolism. These results provide insight into the biological mechanisms of insulin resistance and β-cell dysfunction, identifying early pathophysiological changes to facilitate the identification of relevant biomarkers to improve diagnosis and treatment of T2D.

Acknowledgments

We thank the investigators, staff, and participants of the studies for valuable contributions.

Financial Support: This research was supported by the IRAS-FS through funding provided by the National Institutes Health Grants HL060944 (to L.E.W.), HL061019 (to J.M.N.), HL060919, DK085175 (to L.E.W.), and HG007112 (to D.W.B.).

Correspondence and Reprint Requests: Nicholette D. Palmer, PhD, Department of Biochemistry, 1 Medical Center Boulevard, Winston-Salem, North Carolina 27157. E-mail: nallred@wakehealth.edu.

Disclosure Summary: The authors have nothing to disclose.

References

1. Kahn SE, Prigeon RL, McCulloch DK, Boyko EJ, Bergman RN, Schwartz MW, Neifing JL, Ward WK, Beard JC, Palmer JP. Quantification of the relationship between insulin sensitivity and β-cell function in human subjects. Evidence for a hyperbolic function. *Diabetes*. 1993;**42**(11):1663–1672.
2. Matthews DR, Hosker JP, Rudenski AS, Naylor BA, Treacher DF, Turner RC. Homeostasis model assessment: insulin resistance and β-cell function from fasting plasma glucose and insulin concentrations in man. *Diabetologia*. 1985;**28**(7):412–419.
3. Song Y, Manson JE, Tinker L, Howard BV, Kuller LH, Nathan L, Rifai N, Liu S. Insulin sensitivity and insulin secretion determined by homeostasis model assessment and risk of diabetes in a multiethnic cohort of women: the Women's Health Initiative Observational Study. *Diabetes Care*. 2007;**30**(7):1747–1752.
4. DeFronzo RA, Tobin JD, Andres R. Glucose clamp technique: a method for quantifying insulin secretion and resistance. *Am J Physiol*. 1979;**237**(3):E214–E223.
5. Saad MF, Anderson RL, Laws A, Watanabe RM, Kades WW, Chen YD, Sands RE, Pei D, Savage PJ, Bergman RN. A comparison between the minimal model and the glucose clamp in the assessment of insulin sensitivity across the spectrum of glucose tolerance. Insulin Resistance Atherosclerosis Study. *Diabetes*. 1994; **43**(9):1114–1121.
6. Beard JC, Bergman RN, Ward WK, Porte D Jr. The insulin sensitivity index in nondiabetic man. Correlation between clamp-derived and IVGTT-derived values. *Diabetes*. 1986; **35**(3):362–369.
7. Bergman RN, Prager R, Volund A, Olefsky JM. Equivalence of the insulin sensitivity index in man derived by the minimal model method and the euglycemic glucose clamp. *J Clin Invest*. 1987; **79**(3):790–800.
8. Korytkowski MT, Berga SL, Horwitz MJ. Comparison of the minimal model and the hyperglycemic clamp for measuring insulin sensitivity and acute insulin response to glucose. *Metabolism*. 1995; **44**(9):1121–1125.
9. Pacini G, Bergman RN. MINMOD: a computer program to calculate insulin sensitivity and pancreatic responsivity from the frequently sampled intravenous glucose tolerance test. *Comput Methods Programs Biomed*. 1986;**23**(2):113–122.
10. Newgard CB. Metabolomics and metabolic diseases: where do we stand? *Cell Metab*. 2017;**25**(1):43–56.
11. Wang TJ, Larson MG, Vasan RS, Cheng S, Rhee EP, McCabe E, Lewis GD, Fox CS, Jacques PF, Fernandez C, O'Donnell CJ, Carr SA, Mootha VK, Florez JC, Souza A, Melander O, Clish CB, Gerszten RE. Metabolite profiles and the risk of developing diabetes. *Nat Med*. 2011;**17**(4):448–453.
12. Palmer ND, Stevens RD, Antinozzi PA, Anderson A, Bergman RN, Wagenknecht LE, Newgard CB, Bowden DW. Metabolomic profile associated with insulin resistance and conversion to diabetes in the Insulin Resistance Atherosclerosis Study. *J Clin Endocrinol Metab*. 2015;**100**(3):E463–E468.
13. Newgard CB, An J, Bain JR, Muehlbauer MJ, Stevens RD, Lien LF, Haqq AM, Shah SH, Arlotto M, Slentz CA, Rochon J, Gallup D, Ilkayeva O, Wenner BR, Yancy WS Jr, Eisenson H, Musante G, Surwit RS, Millington DS, Butler MD, Svetkey LP. A branched-chain

amino acid-related metabolic signature that differentiates obese and lean humans and contributes to insulin resistance. *Cell Metab*. 2009; **9**(4):311–326.
14. Rhee EP, Cheng S, Larson MG, Walford GA, Lewis GD, McCabe E, Yang E, Farrell L, Fox CS, O'Donnell CJ, Carr SA, Vasan RS, Florez JC, Clish CB, Wang TJ, Gerszten RE. Lipid profiling identifies a triacylglycerol signature of insulin resistance and improves diabetes prediction in humans. *J Clin Invest*. 2011;**121**(4):1402–1411.
15. Henkin L, Bergman RN, Bowden DW, Ellsworth DL, Haffner SM, Langefeld CD, Mitchell BD, Norris JM, Rewers M, Saad MF, Stamm E, Wagenknecht LE, Rich SS. Genetic epidemiology of insulin resistance and visceral adiposity. The IRAS Family Study design and methods. *Ann Epidemiol*. 2003;**13**(4):211–217.
16. Steil GM, Volund A, Kahn SE, Bergman RN. Reduced sample number for calculation of insulin sensitivity and glucose effectiveness from the minimal model. Suitability for use in population studies. *Diabetes*. 1993;**42**(2):250–256.
17. Bergman RN, Ider YZ, Bowden CR, Cobelli C. Quantitative estimation of insulin sensitivity. *Am J Physiol*. 1979;**236**(6):E667–E677.
18. Bergman RN, Finegood DT, Ader M. Assessment of insulin sensitivity in vivo. *Endocr Rev*. 1985;**6**(1):45–86.
19. Levy JC, Matthews DR, Hermans MP. Correct homeostasis model assessment (HOMA) evaluation uses the computer program. *Diabetes Care*. 1998;**21**(12):2191–2192.
20. Almasy L, Blangero J. Multipoint quantitative-trait linkage analysis in general pedigrees. *Am J Hum Genet*. 1998;**62**(*5*): 1198–1211.
21. Palmer ND, Wagenknecht LE, Langefeld CD, Wang N, Buchanan TA, Xiang AH, Allayee H, Bergman RN, Raffel LJ, Chen YD, Haritunians T, Fingerlin T, Goodarzi MO, Taylor KD, Rotter JI, Watanabe RM, Bowden DW. Improved performance of dynamic measures of insulin response over surrogate indices to identify genetic contributors of type 2 diabetes: the GUARDIAN Consortium. *Diabetes*. 2016;**65**(7):2072–2080.
22. Gall WE, Beebe K, Lawton KA, Adam KP, Mitchell MW, Nakhle PJ, Ryals JA, Milburn MV, Nannipieri M, Camastra S, Natali A, Ferrannini E; RISC Study Group. α-Hydroxybutyrate is an early biomarker of insulin resistance and glucose intolerance in a nondiabetic population. *PLoS One*. 2010;**5**(*5*):e10883.
23. Lee S, Zhang C, Kilicarslan M, Piening BD, Bjornson E, Hallström BM, Groen AK, Ferrannini E, Laakso M, Snyder M, Blüher M, Uhlen M, Nielsen J, Smith U, Serlie MJ, Boren J, Mardinoglu A. Integrated network analysis reveals an association between plasma mannose levels and insulin resistance. *Cell Metab*. 2016;**24**(1): 172–184.
24. Menni C, Fauman E, Erte I, Perry JR, Kastenmüller G, Shin SY, Petersen AK, Hyde C, Psatha M, Ward KJ, Yuan W, Milburn M, Palmer CN, Frayling TM, Trimmer J, Bell JT, Gieger C, Mohney RP, Brosnan MJ, Suhre K, Soranzo N, Spector TD. Biomarkers for type 2 diabetes and impaired fasting glucose using a nontargeted metabolomics approach. *Diabetes*. 2013;**62**(12):4270–4276.
25. Suhre K, Meisinger C, Döring A, Altmaier E, Belcredi P, Gieger C, Chang D, Milburn MV, Gall WE, Weinberger KM, Mewes HW, Hrabé de Angelis M, Wichmann HE, Kronenberg F, Adamski J, Illig T. Metabolic footprint of diabetes: a multiplatform metabolomics study in an epidemiological setting. *PLoS One*. 2010;**5**(11): e13953.
26. Fiehn O, Garvey WT, Newman JW, Lok KH, Hoppel CL, Adams SH. Plasma metabolomic profiles reflective of glucose homeostasis in non-diabetic and type 2 diabetic obese African-American women. *PLoS One*. 2010;**5**(12):e15234.
27. Galgani JE, Moro C, Ravussin E. Metabolic flexibility and insulin resistance. *Am J Physiol Endocrinol Metab*. 2008;**295**(*5*): E1009–E1017.
28. Lingvay I, Esser V, Legendre JL, Price AL, Wertz KM, Adams-Huet B, Zhang S, Unger RH, Szczepaniak LS. Noninvasive quantification of pancreatic fat in humans. *J Clin Endocrinol Metab*. 2009;**94**(10): 4070–4076.
29. Singh B, Saxena A. Surrogate markers of insulin resistance: a review. *World J Diabetes*. 2010;**1**(2):36–47.
30. Nguyen D, Samson SL, Reddy VT, Gonzalez EV, Sekhar RV. Impaired mitochondrial fatty acid oxidation and insulin resistance in aging: novel protective role of glutathione. *Aging Cell*. 2013; **12**(3):415–425.
31. Sener A, Best LC, Yates AP, Kadiata MM, Olivares E, Louchami K, Jijakli H, Ladrière L, Malaisse WJ. Stimulus-secretion coupling of arginine-induced insulin release: comparison between the cationic amino acid and its methyl ester. *Endocrine*. 2000;**13**(3):329–340.
32. Newsholme P, Brennan L, Rubi B, Maechler P. New insights into amino acid metabolism, β-cell function and diabetes. *Clin Sci (Lond)*. 2005;**108**(3):185–194.
33. Abbasi F, Asagmi T, Cooke JP, Lamendola C, McLaughlin T, Reaven GM, Stuehlinger M, Tsao PS. Plasma concentrations of asymmetric dimethylarginine are increased in patients with type 2 diabetes mellitus. *Am J Cardiol*. 2001;**88**(10):1201–1203.
34. Stühlinger MC, Abbasi F, Chu JW, Lamendola C, McLaughlin TL, Cooke JP, Reaven GM, Tsao PS. Relationship between insulin resistance and an endogenous nitric oxide synthase inhibitor. *JAMA*. 2002;**287**(11):1420–1426.
35. Manning AK, Hivert MF, Scott RA, Grimsby JL, Bouatia-Naji N, Chen H, Rybin D, Liu CT, Bielak LF, Prokopenko I, Amin N, Barnes D, Cadby G, Hottenga JJ, Ingelsson E, Jackson AU, Johnson T, Kanoni S, Ladenvall C, Lagou V, Lahti J, Lecoeur C, Liu Y, Martinez-Larrad MT, Montasser ME, Navarro P, Perry JR, Rasmussen-Torvik LJ, Salo P, Sattar N, Shungin D, Strawbridge RJ, Tanaka T, van Duijn CM, An P, de Andrade M, Andrews JS, Aspelund T, Atalay M, Aulchenko Y, Balkau B, Bandinelli S, Beckmann JS, Beilby JP, Bellis C, Bergman RN, Blangero J, Boban M, Boehnke M, Boerwinkle E, Bonnycastle LL, Boomsma DI, Borecki IB, Böttcher Y, Bouchard C, Brunner E, Budimir D, Campbell H, Carlson O, Chines PS, Clarke R, Collins FS, Corbatón-Anchuelo A, Couper D, de Faire U, Dedoussis GV, Deloukas P, Dimitriou M, Egan JM, Eiriksdottir G, Erdos MR, Eriksson JG, Eury E, Ferrucci L, Ford I, Forouhi NG, Fox CS, Franzosi MG, Franks PW, Frayling TM, Froguel P, Galan P, de Geus E, Gigante B, Glazer NL, Goel A, Groop L, Gudnason V, Hallmans G, Hamsten A, Hansson O, Harris TB, Hayward C, Heath S, Hercberg S, Hicks AA, Hingorani A, Hofman A, Hui J, Hung J, Jarvelin MR, Jhun MA, Johnson PC, Jukema JW, Jula A, Kao WH, Kaprio J, Kardia SL, Keinanen-Kiukaanniemi S, Kivimaki M, Kolcic I, Kovacs P, Kumari M, Kuusisto J, Kyvik KO, Laakso M, Lakka T, Lannfelt L, Lathrop GM, Launer LJ, Leander K, Li G, Lind L, Lindstrom J, Lobbens S, Loos RJ, Luan J, Lyssenko V, Mägi R, Magnusson PK, Marmot M, Meneton P, Mohlke KL, Mooser V, Morken MA, Miljkovic I, Narisu N, O'Connell J, Ong KK, Oostra BA, Palmer LJ, Palotie A, Pankow JS, Peden JF, Pedersen NL, Pehlic M, Peltonen L, Penninx B, Pericic M, Perola M, Perusse L, Peyser PA, Polasek O, Pramstaller PP, Province MA, Räikkönen K, Rauramaa R, Rehnberg E, Rice K, Rotter JI, Rudan I, Ruokonen A, Saaristo T, Sabater-Lleal M, Salomaa V, Savage DB, Saxena R, Schwarz P, Seedorf U, Sennblad B, Serrano-Rios M, Shuldiner AR, Sijbrands EJ, Siscovick DS, Smit JH, Small KS, Smith NL, Smith AV, Stančáková A, Stirrups K, Stumvoll M, Sun YV, Swift AJ, Tönjes A, Tuomilehto J, Trompet S, Uitterlinden AG, Uusitupa M, Vikström M, Vitart V, Vohl MC, Voight BF, Vollenweider P, Waeber G, Waterworth DM, Watkins H, Wheeler E, Widen E, Wild SH, Willems SM, Willemsen G, Wilson JF, Witteman JC, Wright AF, Yaghootkar H, Zelenika D, Zemunik T, Zgaga L, Wareham NJ, McCarthy MI, Barroso I, Watanabe RM, Florez JC, Dupuis J, Meigs JB, Langenberg C; DIAbetes Genetics Replication And Meta-analysis (DIAGRAM) Consortium; Multiple Tissue Human Expression Resource (MUTHER) Consortium. A genome-wide approach accounting for body mass index identifies genetic variants influencing fasting glycemic traits and insulin resistance. *Nat Genet*. 2012;**44**(6):659–669.

36. Lorenzo C, Wagenknecht LE, Rewers MJ, Karter AJ, Bergman RN, Hanley AJ, Haffner SM. Disposition index, glucose effectiveness, and conversion to type 2 diabetes: the Insulin Resistance Atherosclerosis Study (IRAS). *Diabetes Care*. 2010;**33**(9): 2098–2103.
37. Bojanowska E. Physiology and pathophysiology of glucagon-like peptide-1 (GLP-1): the role of GLP-1 in the pathogenesis of diabetes mellitus, obesity, and stress. *Med Sci Monit*. 2005;**11**(8): RA271–RA278.
38. Lu X, Zhao X, Feng J, Liou AP, Anthony S, Pechhold S, Sun Y, Lu H, Wank S. Postprandial inhibition of gastric ghrelin secretion by long-chain fatty acid through GPR120 in isolated gastric ghrelin cells and mice. *Am J Physiol Gastrointest Liver Physiol*. 2012; **303**(3):G367–G376.
39. Wallin A, Di Giuseppe D, Orsini N, Patel PS, Forouhi NG, Wolk A. Fish consumption, dietary long-chain n-3 fatty acids, and risk of type 2 diabetes: systematic review and meta-analysis of prospective studies. *Diabetes Care*. 2012;**35**(4): 918–929.
40. Wu JHY, Marklund M, Imamura F, Tintle N, Ardisson Korat AV, de Goede J, Zhou X, Yang WS, de Oliveira Otto MC, Kröger J, Qureshi W, Virtanen JK, Bassett JK, Frazier-Wood AC, Lankinen M, Murphy RA, Rajaobelina K, Del Gobbo LC, Forouhi NG, Luben R, Khaw KT, Wareham N, Kalsbeek A, Veenstra J, Luo J, Hu FB, Lin HJ, Siscovick DS, Boeing H, Chen TA, Steffen B, Steffen LM, Hodge A, Eriksdottir G, Smith AV, Gudnason V, Harris TB, Brouwer IA, Berr C, Helmer C, Samieri C, Laakso M, Tsai MY, Giles GG, Nurmi T, Wagenknecht L, Schulze MB, Lemaitre RN, Chien KL, Soedamah-Muthu SS, Geleijnse JM, Sun Q, Harris WS, Lind L, Ärnlöv J, Riserus U, Micha R, Mozaffarian D; Cohorts for Heart and Aging Research in Genomic Epidemiology (CHARGE) Fatty Acids and Outcomes Research Consortium (FORCE). Omega-6 fatty acid biomarkers and incident type 2 diabetes: pooled analysis of individual-level data for 39 740 adults from 20 prospective cohort studies. *Lancet Diabetes Endocrinol*. 2017;**5**(12):965–974.
41. Weir GC, Bonner-Weir S. Five stages of evolving beta-cell dysfunction during progression to diabetes. *Diabetes*. 2004;**53**(Suppl 3):S16–S21.